

# Numerical Investigation of Cycle Cut-off Criterion on System Performance of Thermocline Tank

Karem Elsayed Elfeky, Abubakar Gambo Mohammed, Qiuwang Wang\*

Key Laboratory of Thermo-Fluid Science and Engineering, MOE, Xi'an Jiaotong University, Xi'an, Shaanxi 710049, China  
[wangqw@mail.xjtu.edu.cn](mailto:wangqw@mail.xjtu.edu.cn)

The current paper investigates the cycle cut-off criterion on the thermal performance of the three-layers thermocline thermal energy storage (TES) tank system which is used in concentrating solar power (CSP) plants. The one dimensional transient dispersion-concentric (D-C) scheme is applied to calculate the phase change inside each capsule. Using MATLAB software, the numerical model equations have been figured out. Five different scenarios have been created to investigate the cycle cut-off criterion on the thermal performance of the TES tank. The results indicate that there are two important aspects to assess system performance which are the temperature distribution during the charging/discharging cycles and the time required to achieve equilibrium conditions. These aspects directly affect the overall power and external efficiency of the storage system and play a key role in understanding the system start up properties and provide insight into storage availability when designing the power cycle for CSP applications. It was also noted that the cycle times and the time required to achieve periodic conditions are very sensitive not only to the storage temperature difference but also to the cutting temperature difference. The difference in the duration of the charge cycle and the corresponding discharge cycle can be attributed to the consideration of a similar cut-off standard.

## 1. Introduction

One of the greater important sources of renewable energy is solar energy because, it is free and with time it is inexhaustible, and has been widely used through photovoltaic (PV) or concentrating solar power (CSP) plants (Ju et al., 2017). Thermal energy storage (TES) has attracted considerable attention from researchers around the world because of its effectiveness in terms of efficiency and cost for all applications of solar energy at low, medium and high temperatures (Jiang et al., 2019). Using three different ways the thermal energy can be stored: thermochemical, sensible, and latent heat storage. At present, thermochemical storage of heat is still undergoing laboratory investigations in labs, while sensible heat storage has been widely spread in industrial applications (Jiang et al., 2019). However, storage energy by sensible heat faces a major problem namely low energy storage density. Latent heat storage as TES technology is better than sensible heat storage because it has a high storage density and can store/recover energy at the low difference in temperature between the heat transfer fluid (HTF) and the PCMs capsules (Elfeky et al., 2019).

Phase change materials (PCMs) are one of the recommended ways to store latent thermal energy due to its efficiency and ability to charging and discharging energy in the shortest time (Ling et al., 2015). Recent researches have attempted to use high melting temperature PCMs for thermocline tank in CSP plants; many studies investigated different ways which can improve the charging and discharging efficiency of the thermocline tank by using a single PCM layer with different melting temperatures (Aldoss et al., 2014), cascaded PCMs (Elfeky et al., 2018), and combined sensible latent heat TES (Ahmed et al., 2019).

Most recently, Gracia et al. (2016) reviewed and discussed the different numerical methodologies available in the literature which are used to predict the performance of latent packed bed the TES systems. Singh et al. (2013) presented the exergy analysis for packed bed TES system and compare this to PCM-based storage. Esence et al. (2017) investigated a review on experience feedback and numerical modelling of packed-bed TES systems. In the first part, presented the most representative setups and their experience feedback. In the last part, compared and presented various numerical models used to predict packed-bed storage performances. Flueckiger et al. (2014) investigated the starting point for PCM melting point selection. The studies demonstrated

that there is a severe improvement in system output, utilization, and a plant's capacity factor when the phase transition temperature falls between the charging ( $\theta_c$ ) and discharging ( $\theta_d$ ) cut-off temperatures. Referring to the above studies and the developed dispersion-concentric (D-C) model in lab previous work (Elfeky et al., 2019), it can be found that, the cycle cut-off criterion of the system during charging and discharging would be remarkable on the thermal behaviour of the TES tank system, especially at the lower and upper part of the tank. However, the thermal behaviour of the TES tank which consists of single layers of PCMs, using different numerical approach has been widely investigated over the past years but, the investigation of the cycle cut-off criterion for three-layers thermocline tank during charging and discharging cycles has not been studied. In the present work, the thermal behaviour of the three-layers TES tank is numerically investigated at a different cycle cut-off criterion for charging and discharging cycles. Both of the temperature distribution, charging/discharging time, energy stored/recovered, overall efficiency, exergy efficiency and capacity/utilization ratio are studied to understand and evaluate the thermal behaviour of the TES tank.

## 2. Numerical formulation

The schematic diagram of the TES tank system which used three layers of the PCMs with different thermo-physical properties is shown in Figure 1. The tank is filled with three different layers of PCMs with an equal radius and at different melting points. The HTF passes through the spaces which exist between the capsules.

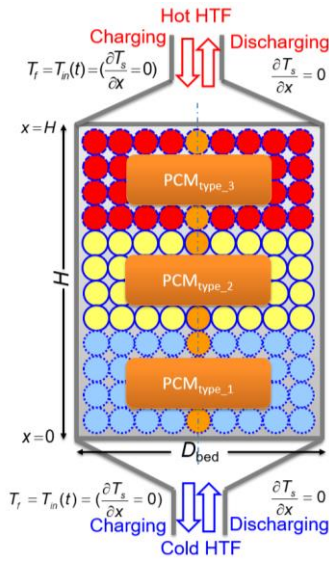


Figure 1: Schematic diagram of packed bed thermal storage system

In the present study, making comparison between the system performance with change in the cut-off temperature difference. The cut-off temperature difference was changed from 5 °C to 80 °C while using HTF as the HTF. The TES tank system performance was investigated with respect to the change in the cut-off temperature difference. The cut-off criteria for the charging and discharging processes are applied. These threshold values are characterized by a normalized temperature, which is expressed as:

$$\theta = \frac{T_{PCM} - T_{c,t}}{T_{h,t} - T_{c,t}} \quad (1)$$

where  $T_{h,t}$  and  $T_{c,t}$  are the HTF inlet temperature during charge/discharge cycles.

Table 1: Cases summary for the cut-off temperature value

Case	Cut-off ( $\Delta T$ )	$\theta_c$	$\theta_d$
Case (A)	-	0.3357	0.7833
Case (B)	5	0.3537	0.7653
Case (C)	10	0.3718	0.7472
Case (D)	15	0.3898	0.7292
Case (E)	20	0.4079	0.7111
Case (F)	25	0.4259	0.6931

The above five different cut-off temperature difference cases are considered as shown in Table 1. Three-stage packed bed PCMs, where the bed is divided equally into three axial-sections, each PCM occupies 1/3 of the bed, each section is filled with different PCM material, PCM<sub>type-1</sub>, PCM<sub>type-2</sub> and PCM<sub>type-3</sub> in sequence. The arrangements are considered in this case based on the PCM melting temperature, high to low (PCM<sub>type-3</sub>, PCM<sub>type-2</sub>, PCM<sub>type-1</sub>). The thermophysical properties of the PCMs which have been applied in this paper are demonstrated in Table 2, as mentioned in (Liu, 2015).

Table 2: PCMs thermo-physical properties

Arrangement	PCM <sub>type-1</sub>	PCM <sub>type-2</sub>	PCM <sub>type-3</sub>
Melting temperature (°C)	382.1	439.8	505
Solidification temperature (°C)	382.1	439.8	505
Latent heat of fusion (kJ/kg)	197.6	214.9	344
Latent heat of solidification (kJ/kg)	197.6	214.9	344
Solid density (kg/m <sup>3</sup> )	2118	2109	2266
Liquid density (kg/m <sup>3</sup> )	1607	1604	2160
Solid thermal conductivity (W/m-°C)	1.0	1.0	2
Liquid thermal conductivity (W/m-°C)	1.0	1.0	1.885
Solid specific heat capacity (J/kg-°C)	928	1005	1338.88
Liquid specific heat capacity (J/kg-°C)	1035	1096	1757.28

## 2.1 Model description

In the present study, the (D-C) numerical model is used to study the dynamic behaviour of the TES tank and explain how the HTF travels through the packing region. The thermocline TES tank in this model is considered as a porous material consisting of separate capsules of the PCMs (Elfeky et al., 2018). The (D-C) model is used because only this approach solves the thermal distribution inside solid capsules. The phase change phenomena of PCM inside the capsules are analysed by the apparent heat capacity method. The assumptions below are as follows:

- 1) The inner and outer surface of the tank is completely insulated.
- 2) The HTF flows from the top inlet port into the bottom outlet port during charging and vice versa during discharging.
- 3) The energy lost from two ends of the thermocline tank is ignored due to its very small value (Elfeky et al., 2018).
- 4) The thermophysical characteristics of the HTF are determined on the basis of the inlet and exit temperature,  $T_{ave} = (T_{in} + T_{ex}) / 2$  (Elfeky et al., 2018).
- 5) The radiation heat transfer and heat generated within the thermocline TES tank have been neglected.

The mathematical equations of the current numerical model that describe the heat transfer process between both the HTF and PCMs capsules are resolved based on the assumptions mentioned above: For the HTF:

$$\varepsilon \rho_f c_{p,f} \frac{\partial T_f}{\partial t} + \varepsilon u_f \rho_f c_{p,f} \frac{\partial T_f}{\partial X} = \varepsilon \lambda_f \frac{\partial^2 T_f}{\partial X^2} + h_f (T_s - T_f) + h_w (T_w - T_f) \quad (2)$$

where  $\varepsilon$  is average bed porosity,  $\rho_f$  is the HTF density,  $c_{p,f}$  is specific heat capacity of the HTF,  $u_f$  is the HTF inlet velocity,  $T_f$  is the temperature of HTF,  $T_s$  is the temperature of the PCM,  $T_w$  is the tank wall temperature,  $h_f$  is the volumetric heat transfer coefficient between fluid and solid,  $h_w$  is the volumetric heat transfer coefficient between tank and ambience,  $\lambda_f$  is the thermal conductivity of the HTF.

For the PCMs capsules:

$$(1 - \varepsilon) \rho_s c_{p,s} \frac{\partial T_s}{\partial t} = (1 - \varepsilon) \lambda_s \frac{\partial^2 T_s}{\partial X^2} + h_f (T_f - T_s) \quad (3)$$

where  $\rho_s$  is the PCM density,  $c_{p,s}$  is specific heat capacity of the PCM,  $\lambda_s$  is the thermal conductivity of the PCM. The distribution of the temperature on the PCM capsule surface can be determined as follows:

$$\rho_s c_{p,s} \frac{\partial T_p}{\partial t} = \frac{1}{r^2} \frac{\partial}{\partial r} \left( \lambda_s r^2 \frac{\partial T_p}{\partial r} \right) \quad (4)$$

where  $r$  is radius of PCM capsule.

## 2.2 Numerical approach

The packing region of the thermocline tank is sectioned to an equal number of control volumes. The axial and the radial direction have been divide into an equal number of sections ( $N_x$ ) and ( $R_x$ ), for all the current studied cases as demonstrated in Figure 1. By directly approximating the finite difference way within the fully implicit scheme, the (D-C) model equations that characterize the rate of heat transfer in between the PCMs capsules and the HTF are solved using MATLAB. The First-order upwind method is used to solve both of the advective and temporal terms in the mathematical equation Eq(2), simultaneously; the second-order central difference approach is used to solve the diffusion term. At the start of charging and discharging cycles, the temperature distribution of PCMs capsules and HTF is determined by the initial and boundary conditions, and then the (D-C) model equations are solved simultaneously.

## 2.3 Performance analysis

The performance metrics in terms of first-law, second-law efficiencies, capacity ratio, and utilization ratio provide the general measurement for TES design and analysis of the thermocline tank. All these parameters have been defined in lab previous work (Elfeky et al., 2018).

## 3. Results and discussion

In the present work, the thermal behavior of the TES thermocline tank is one of the important parameters for determining the power generation and the CSP efficiency. The process of TES in the thermocline tank keeps the CSP plants in operation, the heat transfer process inside this tank during the charging/discharging cycles is of fundamental importance and will be studied in detail in this research.

### 3.1 Temperature profiles in packed bed

Figures 2 shows the HTF temperature profile along the bed, after 300 min for charging and discharging cycles. It is clear that the behaviour of the HTF temperature distribution in the bed is affected by cut-off temperature difference. The studies show that there is a severe improvement in temperature profile during charging discharging process when the cut-off temperature increase. In case (F), the HTF temperature distribution matches the PCM-temperature profile along the bed better. This improves the heat transfer process, and increases the system dynamic performance.

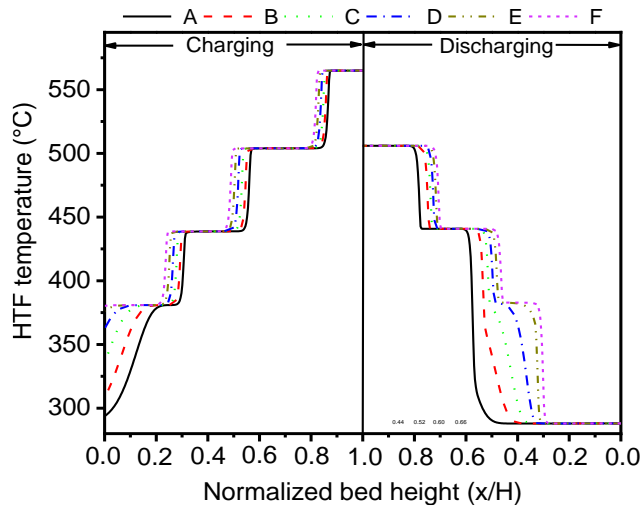


Figure 2: PCM-temperature profile along the bed after 300 min of charging/discharging cycle

The corresponding HTF temperature profiles along the bed are shown in Figures 3a, after steady state of charging and discharging process. During charging cycle, case (F) is the fastest to charge (melt), the HTF temperature is the highest, followed by case (E) then the worst one case (A). During discharge process, the fastest to discharge (solidify) is case (A), showing the lowest HTF temperature profile. This explains why case (F) maintains high performance both in charging and in discharging cycle.

Figures 3b shows the exit temperature of the HTF during charging and discharging cycles. From this figure, it may be observed that with increasing value of the cut-off temperature difference, the durations of both the charge and the discharge cycles increase. This might be expected as increasing cut-off temperature difference

allows for the tank to operate for a longer duration. As might also be expected, the storage capacity of the tank also increases with the cut-off temperature difference as in case (F).

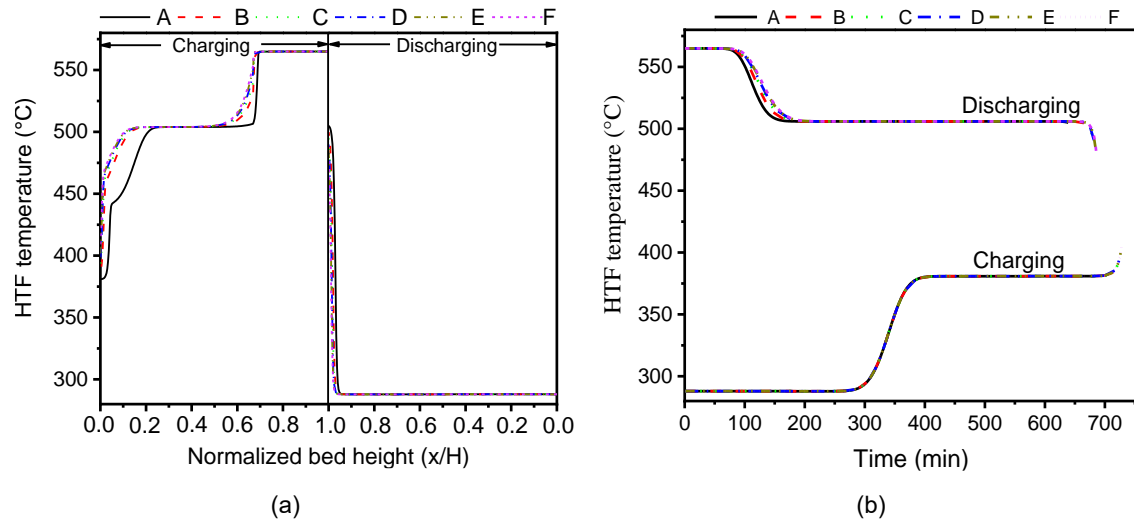


Figure 3: Temperature distribution for: (a) HTF along the bed at the final state and (b) HTF at the bed exit section for charging and discharging cycles

### 3.2 Performance parameters

The performance metrics in terms of first-law, second-law efficiencies, capacity ratio and utilization ratio are used to analysis and investigate the thermal performance for cases study. Figure 5a shows the variations in the overall energy efficiency, charging efficiency and discharging efficiency for all case. The case (F) design attains the highest performance, case (E), the second and case (A), the worst in row. Figure 5b shows the variations in the utilization ratio, capacity ratio and overall exergy efficiency for the all cases. The case (F) design attains the highest performance, case (E), the second and case (A), the worst in row. It is found that energy and exergy efficiencies vary between 39.2 - 73.6 % and 35.1 - 70.6 %, for four cases. Energy efficiency was found higher than the exergy efficiency for different cases. Energy efficiency was calculated based on the total quantity of energy transferred throughout the system. On the other hand, the exergy efficiency quantified only useful amount of energy. To increase the exergy efficiency, it is necessary to prevent the destruction of exergy during discharging cycle.

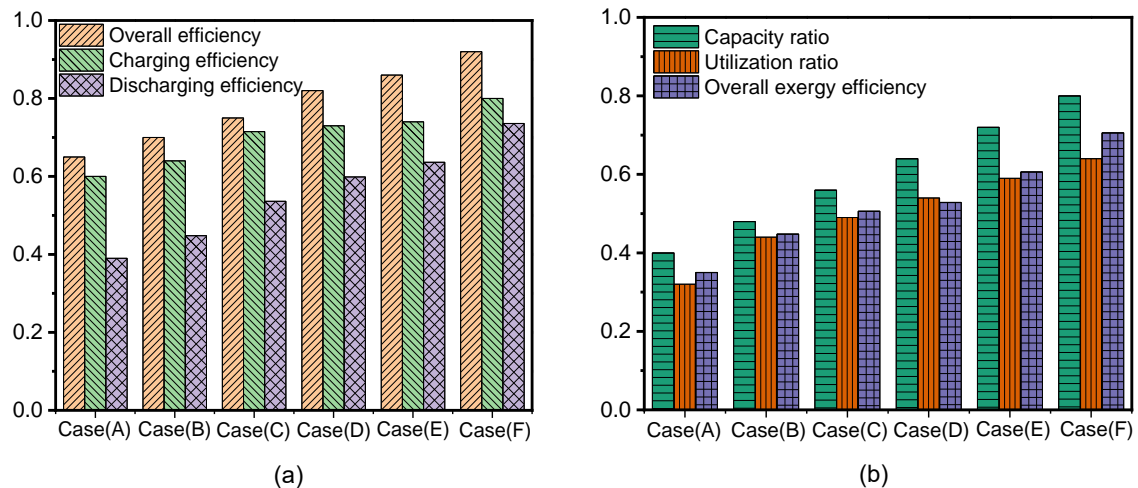


Figure 4: Performance parameters for the four cases study: (a) Energy efficiency and (b) Utilization ratio, capacity ratio and overall exergy efficiency

#### 4. Conclusions

A dispersion-concentric model for a packed bed latent heat thermal energy storage using spherical capsules is developed in the present study to predict the thermal behaviour of the system at different cases. The effect of variation in important system parameters like the cut-off criterion on system performance was investigated. Then, the performance of five cases are analysed by using the performance metrics in terms of first-law, second-law efficiencies, capacity ratio and utilization ratio. The results show that the temperature profiles during charging discharging cycles and the overall energy efficiency depended upon the storage temperature difference, but not on the initial conditions. The overall efficiency, second-law efficiencies, capacity ratio and utilization ratio for case (F) are higher by 13.7 %, 14.2 %, 7.8 %, and 10.7 % than case (E). Besides, the overall efficiency, second-law efficiencies, capacity ratio and utilization ratio for case (F) are higher by 47.2 %, 50.8 %, 48.58 %, and 50.8 % than case (A). The effect of the temperature difference between the hot fluid and the cold fluid in the storage system has a great impact on system performance (i.e. the system takes longer to attain cyclic behaviour even when the duration of individual cycles is smaller for higher temperature differences). The difference in the durations of the charge cycle and its corresponding discharge cycle can be attributed to the consideration of similar cycle cut-off criterion and thermal losses to the ambient. The storage capacity of the tank is highly sensitive to both the cycle cut-off criteria and the storage temperature difference.

#### Acknowledgments

This work is financially supported by the National Natural Science Foundation of China (Grant No. 51536007), the National Natural Science Foundation of China (NSFC) / Research Grants Council (RGC) Joint Research Scheme (Grant No. 51861165105), the Foundation for Innovative Research Groups of the National Natural Science Foundation of China (No.51721004) and the 111 Project (B16038).

#### References

- Aldoss T. K., Rahman M. M., 2014, Comparison between the single-PCM and multi-PCM thermal energy storage design, *Energy Conversion and Management*, 83, 79 - 87.
- Ahmed N., Elfeky K. E., Qaisrani M. A., Wang Q., 2019, Numerical characterization of thermocline behavior of combined sensible-latent heat storage tank using brick manganese rod structure impregnated with PCM capsules, *Solar Energy*, 180, 243 - 256.
- Esence T., Bruch A., Molina S., Stutz B., Fourmigue J. F., 2017, A review on experience feedback and numerical modeling of packed-bed thermal energy storage systems, *Solar Energy*, 153, 628 - 654.
- Elfeky K. E., Ahmed N., Wang Q., 2018, Numerical comparison between single PCM and multi-stage PCM based high temperature thermal energy storage for CSP tower plants, *Applied Thermal Engineering*, 139, 609 - 622.
- Elfeky K. E., Li X., Ahmed N., Lu L., Wang Q., 2019, Optimization of thermal performance in thermocline tank thermal energy storage system with the multilayered PCM(s) for CSP tower plants, *Applied Energy*, 243, 175 - 190.
- Flueckiger S. M., Garimella S. V., 2014, Latent heat augmentation of thermocline energy storage for concentrating solar power-a system-level assessment, *Applied Energy*, 116, 278-287.
- Gracia A. de. Cabeza L. F., 2016, Numerical simulation of a PCM packed bed system: A review, *Solar Energy* 69, 1055-1063.
- Jiang Y., Liu M., Sun Y., 2019, Review on the development of high temperature phase change material composites for solar thermal energy storage, *Solar Energy Materials and Solar Cells*, 203, 110164.
- Ju X., Xu C., Hu Y., Han X., Wei G., Du X., 2017, A review on the development of photovoltaic/concentrated solar power (PV-CSP) hybrid systems, *Solar Energy Materials and Solar Cells*, 161, 305 - 327.
- Liu M., Gomez J., Turchi C., Tay N., Saman W., Bruno F., 2015, Determination of thermo-physical properties and stability testing of high-temperature phase-change materials for CSP applications, *Solar Energy Materials and Solar Cells*, 139, 81 - 87.
- Ling Z., Chen J., Xu T., Fang X., Gao X., Zhang Z., 2015, Thermal conductivity of an organic phase change material/expanded graphite composite across the phase change temperature range and a novel thermal conductivity model, *Energy conversion and management*, 102, 202 - 208.
- Singh H., Saini R. P., Saini J. S., 2013, Performance of a packed bed solar energy storage system having large sized elements with low void fraction, *Solar Energy*, 87, 22 - 34.